EPSC Abstracts
Vol. 10, EPSC2015-640, 2015
European Planetary Science Congress 2015

A numerical model of the physical and chemical evolution of Vesta.

H. Mizzon[1], M. Monnereau[1], M.J. Toplis[1], T.H. Prettyman[2], H.Y. McSween[3], C.A. Raymond[4], C.T. Russell[5], [1]Université de Toulouse - Institut de Recherche en Astrophysique et Planétologie, Toulouse, France (hugau.mizzon@irap.omp.eu), [2]Planetary Science Institute, Tucson, AZ, [3]University of Tennessee, Knoxville, TN, [4]Jet Propulsion Laboratory, Pasadena, CA, [5]University of California Los Angeles, CA.

1. Introduction

Vesta is a 262 km radius asteroid that has been proposed as the parent body of the Howardite-Eucrite-Diogenite family of meteorites. The observations of the Dawn spacecraft confirm the idea that this protoplanet underwent magmatic differentiation, providing evidence for regions of the upper crust rich in basaltic (eucritic) lithologies, while regions that have experienced excavation related to large impacts (i.e. Rheasilvia) are richer in pyroxene-dominated (diogenitic) lithologies [1,2]. One of the most striking results of the Dawn mission is the absence of olivine at the near-surface, even in the deep Rheasiliva basin. This observation has been used to question the chondritic nature of bulk Vesta and/or question its status as an intact protoplanet [3].

From a geochemical point of view, the HED meteorites are consistent with chondritic precursors [4], but petrological models have met difficulties explaining both eucrites and diogenites in a unified way [5]. These models comprise two extreme endmember scenarios: the first considers the partial melting of the primitive mantle of Vesta, followed by melt extraction [6], while the second involves the solidification of an initially entirely molten magma ocean [7]. In the latter case, major-element chemistry of eucrites and diogenites can be reproduced [7], but not the extreme range of trace element concentrations observed in diogenites [8]. More importantly, the physics of melt migration seems to preclude the existence of a global magma ocean, assuming that ^{26}Al is the only heat source capable of extensively producing melt in early small bodies. This is because plagioclase is one of the first phases to melt, thus early formed liquids are Al-rich. Rapid migration of such liquids redistributes ^{26}Al, limiting melt production where liquid has been lost [9,10]. This idea was explored by [11], who qualitatively suggested that the first melts formed would migrate to the surface (as eucrites), while the lower mantle would become enriched in refractory olivine through its downward compaction. This last point potentially explains the lack of this mineral near Vesta's surface. The aim of work presented here is to quantitatively explore this idea by computing the mineralogy as a function of depth and time, using a set of numerical solutions of conservative equations and an appropriate phase diagram.

2. The Model

Our model is based on the idea that mineralogy can be monitored by coupling compaction equations with a phase diagram [*e.g.* 12]. For modelling Vesta, we assumed instantaneous accretion, an initial temperature of 292K and a homogeneous composition derived from H type chondrites [4]. Each time step involves the following: 1) Coupled mass and momentum conservation equations computing the proportion of the different phases (solid, liquid) for all components considered (iron metal, iron sulfide, olivine, pyroxene and anorthite). These equations [13] describe the two phase flow between a high viscosity matrix (a mixture of solid silicates and metal here), and a low viscosity mobile fluid (molten silicates). 2) Temperature is then solved accounting for ^{26}Al decay with conductive cooling, without considering the effect of latent heat. Knowing the composition and the amount of available energy, a phase diagram provides the equilibrium temperature, the amount of melt, and the compositions of the liquid and solid. 3) The equilibrium temperature and the amount of melt is used to correct the initial estimations of the phase proportions and account for the effect of release or consumption of latent heat on the temperature. This enthalpy method is extensively described by [14], and a similar computation for planetesimals with pure components can be found in [15]. We considered a binary phase diagram for iron metal and iron sulfides. Because the eucrites and diogenites are

volatile depleted, the silicate composition can be well approximated by a set of three minerals: anorthite $CaAl_2Si_2O_8$, olivine $(Fe,Mg)_2SiO_4$ and pyroxene $(Ca,Fe,Mg)_2Si_2O_6$. We have therefore used a simplified forsterite – anorthite - silica phase diagram adapted for the effect of additional iron from [16].

In general liquid moves up towards the surface, locally reaching high concentrations. We assumed that when a critical liquid fraction is attained (taken to be 80%) the layer behaves like a magma ocean (i.e. there is no thermal gradient across the layer). Because the liquid is concentrated in ^{26}Al, this layer thermally erodes the subsurface, thinning the overlying conductive lid. We also make the assumption that the conductive lid is recycled into the magma ocean when its thickness is less than 10 km, taking account of a loss of cohesion by thermal expansion, by impacts, or by the effect of the pressure exerted by the underlying magma ocean.

3. Results

A simulation run for our bulk composition and an accretion time 0.7 Myr after CAI formation, shows that the first melt reaches the surface within 1.2 Ma of CAI formation, a time at which the lower mantle has reached a melting degree of barely 10%. Melting in the lower mantle proceeds until it is completely depleted in aluminum. For this reason silicate melting stops at about 4.0 Myr after CAIs, leaving an olivine residue with only a few percent of pyroxenes in the lower mantle. In the meantime, near the surface a competition between heating by ^{26}Al and magma-ocean cooling takes place. The liquid layer is fed both by liquid coming from below and by local ^{26}Al overheating. When the melt fraction is sufficient, the composition is stirred and homogenized in this convective layer, but more importantly, the surface lid is regularly recycled by volcanism, which significantly cools the magma ocean and makes it crystalize. This process repeats itself until the energy provided by ^{26}Al decay cannot produce further melt. When the magma ocean cools to the point where convection is stopped, the more refractory pyroxenes crystallize at its base while the surface solidifies with a near-eutectic composition. The resulting upper crust is $An_{50}Px_{50}$, which is in good agreement with normative eucrite composition [17]. The underlying rock compositions are 90 – 100% pyroxenes, consistent with diogenites.

In this 1D model the composition of eucrite and diogenite layers and their thickness (Figure 1) are independent of accretion time as long as the latter is < ~0.8 Myr after CAI formation. This does not exclude regional variations of crustal thickness, indicated by geophysical data [18], that may occur due to 3D interactions.

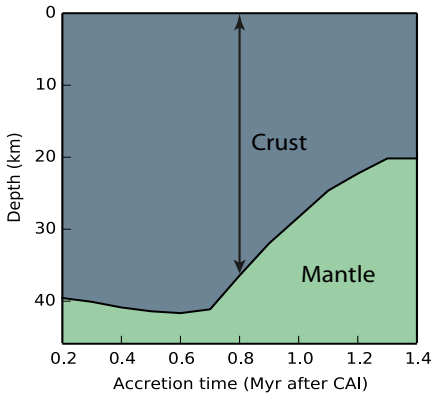

Figure 1: The crust, considered here as the less refractory material brought to the surface by melt migration is represented in grey, while the underlying olivine rich mantle residue is coloured in green. Increasing the accretion time, makes the ^{26}Al energy supply decrease. This results in less melting of the mantle and in a thinner crust.

References: [1] Prettyman T.H. et al (2013), MAPS, 48(11), 2211-2236. [2] DeSanctis et al (2012), Science, 336, 697-700. [3] Clenet H. et al (2013), Nature, 511, 303-305 [4] Toplis et al, (2013), MAPS, 48(11), 2300-2315. [5] Mittlefelhdt D. W., (2012), MAPS, 47(1), 72-98. [6] Stolper E, (1977), 41(5), 587-611 [7] Mandler B. E. and Elkins-Tanton L. T., (2013), MAPS, 48(11), 2333-2349. [8] Barrat J. A. and Yamaguchi A., (2014), MAPS, 49(3), 468-472. [9] Wilson L. and Keil K., (2012), Chemie der Erde, 72, 289-321 [10] Moskovitz N. and Gaidos E., (2011), MAPS, 46(6), 903-918. [11] Neumann et al, (2014), EPSL, 396, 267-280. [12] Ribe N., (1985), EPSL, 73, 361-376. [13] Bercovici D. and Ricard Y., (2003), GJI, 152, 581-596 [14] Katz F. K., (2008), JPetrol., 49(12), 468-472. [15] Sramek O. et al (2012), Icarus, 217, 339-354. [16] Morse S. A. (1980) *Springer-Verlag.* [17] Delaney J. S., (1984), Proc. Lunar Planet Sci Conf, JGR, 89, 251-288. [18] Raymond C.A. et al. (2015) LPSC.